SAND2007-4993C

DYNAMIC COMPACTION OF SAND

J. L. Brown[1], T.J. Vogler[1], D.E. Grady[2], W. D. Reinhart[1], L.C Chhabildas[1], and T. F. Thornhill[1]

[1]Sandia National Laboratories, Albuquerque NM 87185
[2]Applied Research Associates, Southwest Division, Albuquerque NM 87110

Abstract. The dynamic compaction of sand was investigated experimentally and computationally to stresses of 1.8 GPa. Experiments were performed in the partial compaction regime at impact velocities of approximately 0.25, 0.5, and 0.75 km/s. Multiple velocity interferometry probes were used on the rear surface of a stepped target to obtain an accurate measurement of shock velocity, and impedance matching was used to deduce the shock Hugoniot state. Wave profiles were further examined for estimates of reshock states, and a relationship between stress and rise time of the shock was deduced. Experimental results were used to fit parameters for the P-α and P-λ models for porous materials in CTH.

Keywords: Shock waves, granular materials, dynamic compaction, CTH
PACS: 47.40.-x, 47.40.Nm. Use 2 – 4 terms. Find information and list at http://www.aip.org/pacs .

INTRODUCTION

The dynamic behavior of sand and other granular ceramics is of fundamental importance to a variety of engineering applications, including seismic coupling, planetary science applications, penetration, and the performance of ceramic armors. While the behavior of sand has been studied extensively, its dynamic behavior remains poorly understood. High-quality experimental data is needed for computational simulations of dynamic events involving sand and also to improve our understanding of granular physics. Several models have been proposed to describe the dynamic compaction of porous materials. Among the most widely used are the P-α [1] and P-λ models[2, 3]. Both models have been implemented in the CTH hydrocode, but calibration of the models for different materials has generally not been performed. In this report, we describe a series of experiments to measure the shock behavior of sand in the partially compacted region to stresses of 1.8 GPa. These results are compared to shock data for sand from the literature and are used to obtain parameters for the P-α and P-λ models.

EXPERIMENTAL PROCEDURE

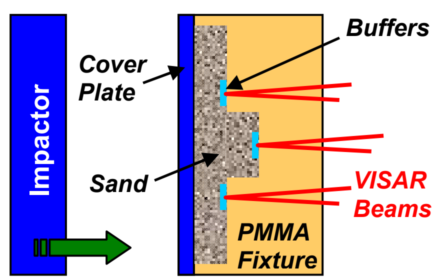

FIGURE 1. Schematic of test fixture illustrating the use of two thicknesses to measure shock velocity.

The current target configuration is a simplified version of one used previously for ceramic powders [4]. A variety of silica sand with an average density of 1.57 g/cm^3 and particle sizes on the order of 200 μm was used in the symmetric impact configuration shown in Fig. 1. The fixture

TABLE 1. Experimental data on dynamic compaction of sand.

V_{impact} (km/s)	ρ_{oo} (g/cm^3)	U_S (km/s)	u_H (km/s)	σ_H (GPa)	ρ_H (g/cm^3)	u_R (km/s)	σ_R (GPa)	ρ_R (g/cm^3)
0.26	1.54	0.79	0.24	0.29	2.21	0.13	2.15	2.25
0.26	1.59	0.80	0.23	0.29	2.22	0.09	1.45	2.32
0.50	1.56	1.21	0.44	0.82	2.44	0.20	3.40	2.57
0.50	1.56	1.31	0.43	0.88	2.32	0.20	3.60	2.43
0.70	1.53	1.56	0.59	1.42	2.47	0.26	4.60	2.70
0.75	1.61	1.76	0.62	1.77	2.49	0.32	5.94	2.63

was designed for use on a 102 mm bore light gas gun. A VISAR system was used to measure the velocity histories at various locations on the rear surface of the stepped target at the PMMA/buffer interfaces. An accurate measurement of the shock velocity was calculated using the arrival times of the velocity histories and the known distance between the target steps.

RESULTS AND DISCUSSION

Hugoniot

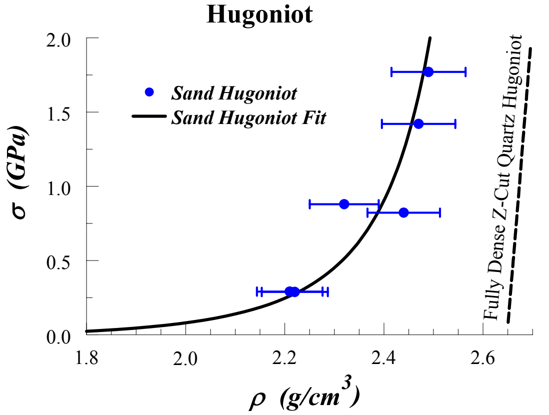

FIGURE 2. Shock response of sand along with a fit of its Hugoniot (Eq. 1).

The Hugoniot data for sand was determined through impedance matching techniques. The shocked state in the cover plate is determined from the symmetry condition for particle velocity and the known Hugoniot of the impactor. When the wave passing through the cover plate reaches the sand, it releases to the Hugoniot for sand. This state is constrained to lie on the cover plate's release path and along a Rayleigh line from the origin with a slope of $\rho_{00}U_s$. Uncertainties of ~3% are expected for σ_H and ~2.5% for ρ_H [4]. Hugoniot data for sand was generated in this manner from 0.3 to 1.8 GPa (Table 1 and Fig. 2). The shock data is represented well over this regime by:

$$U_s = 0.243 + 2.348u_p. \quad (1)$$

The Hugoniot data obtained in the current experiments are compared to other shock data of varying densities and grain sizes [5-8] in Fig. 3. The large scatter in data could be due to differences in materials, experimental techniques, and the inherent difficulties in testing granular materials.

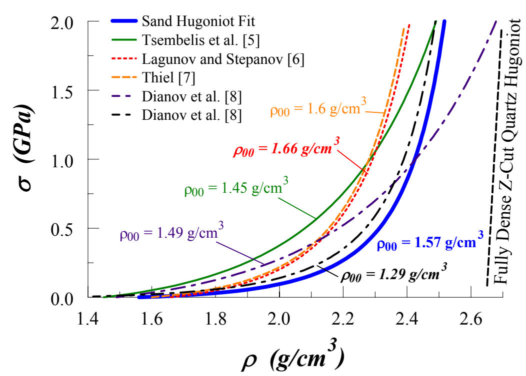

FIGURE 3. Shock response of several varieties of sand along with the Hugoniot of fully dense Z-cut quartz.

Wave Profiles

The measured wave profiles were also used to determine wave rise times and sand reshock states. Rise times were determined as the time between the steady wave's HEL and average peak value. Further, the average peak value of the steady waves can be taken as the shocked state of the PMMA fixture. Impedance matching through the fixture/buffer then buffer/sand interfaces determines the reshock state of the sand. The reshock states were found to be consistently stiffer than the Hugoniot, agreeing well with results seen in tungsten carbide powders [4]. Larger errors, however, are expected in the reshock estimates due to compounding impedance matching errors and the relatively large particle sizes of the sand.

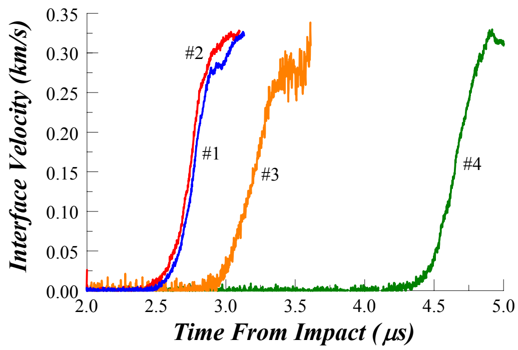

FIGURE 4. Velocity histories from a typical experiment.

Strain Rate

The strain can be calculated from ρ_{00} and ρ_H, and division by the wave rise time yields strain rate. For several fully dense solids, an empirical relationship has been found between strain rate and stress in steady waves of the form

$$\dot{\varepsilon} \propto \sigma^n, \tag{6}$$

where n is found to be approximately 4 [9].

If Eq. 6 is fit to the current experiments, a value of approximately 1 is found for the exponent, n. Similar analysis on ceramic powders produced values for n of 1.0 and 1.2 for TiO_2 [10] and WC [4], respectively.

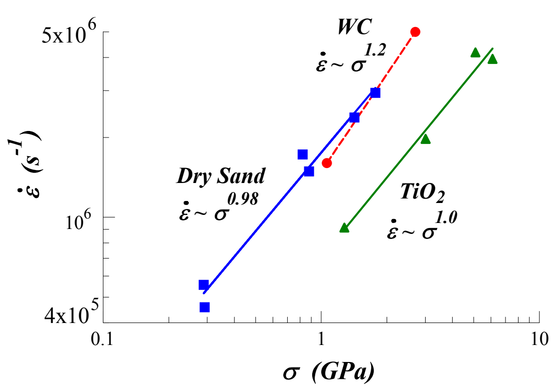

FIGURE 5. Empirical relationship between strain rate and stress in steady waves for several granular materials.

Continuum Models

The P-α model, originally proposed by Hermann [1], provides a simple model for the compaction of porous materials through the utilization of a distention ratio, α, which describes the ratio between the density of the porous material at pressure and the initial density of the solid. While this function can take many forms, the most recent model implemented in CTH is given by

$$\alpha(p) = 1 + (\alpha_0 - 1)\left(\frac{p_s - p}{p_s - p_e}\right)^n, \tag{2}$$

where p_e is the elastic pressure at the onset of compact, p_s is the pressure at which full compaction occurs, and n is a scaling parameter.

More recently, the P-α model has been generalized to accommodate multi-phase mixtures in the form of the P-λ model [2, 3]. The extent of compaction is a combination of the Voigt (iso-strain), ν_V, and Reuss (iso-pressure), ν_R, bounds for the mixture components,

$$\nu_m(p) = \lambda \nu_R(p) + (1-\lambda)\nu_V(p), \tag{3}$$

where λ is a functional expression for the compaction extent. A form of λ found to be applicable to a wide range of transformation processes in heterogeneous media [2] and implemented in CTH is given by

$$\lambda(p) = 1 - e^{-\left(p/p_c\right)^n}, \tag{4}$$

where p_c and n are parameters relating to the ensemble strength on a cellular level and the homogeneity of compaction, respectively [3].

Model Calibrations

The Reuss and Voigt bounds are constant and known, so each Hugoniot state can be used to calculate a corresponding λ, through Eq. 3. These points were utilized in a least squares fit to Eq. 4, resulting in the desired P-λ model parameters. Using this methodology, values of 0.115 GPa, and 0.3 were obtained for p_c and n, respectively. As shown in Fig. 2., the results agree with the experimental data well, typically to within 3%.

Eq. 2, for the P-α model, was also fit to the experimental data. These results, however, were much less convincing, as shown in Fig. 4. An alternative power law form for the model was suggested as

$$\alpha(p) = \left(\frac{p_s}{p}\right)^{1/\eta}. \quad (5)$$

A fit to the form of Eq. 5 yields 3.36 GPa and 13.6 for p_s and η, respectively. These results agree much better with the experiments, as shown in Fig 4.

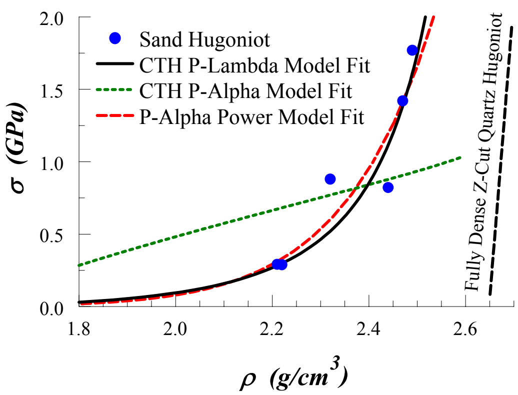

FIGURE 4. P-λ CTH model fit to the experimental data.

CONCLUSIONS

The dynamic compaction of 59% dense dry sand was measured to 1.8 GPa. The experiments were conducted for several states of partial compaction using a novel experimental configuration in which high quality Hugoniot data and time resolved measurements of material behavior are obtained. In addition to the shocked state, a reshock state was also determined from the measured VISAR velocity. The time resolved material response was also examined to obtain initial compaction wave rise times and strain rates. The empirical relationship between strain rate and stress ($\dot{\varepsilon} \sim \sigma^1$) was found to be much different from that of fully dense materials ($\dot{\varepsilon} \sim \sigma^4$) but consistent with other ceramic powders.

The current data set was also used to obtain parameters for computational modeling efforts in CTH using the P-α and P-λ models. While the calibrated P-λ model simulated the experiments to within 3%, the current form of the P-α model was unable to accurately represent the shock response of the sand. Instead, an alternate distention equation in the form of a power-law was found to fit the data very well. Implementation of this form of the equation in CTH should be considered to improve the P-α model.

ACKNOWLEDGEMENTS

Sandia is a multiprogram laboratory operated by Sandia Corporation, a Lockheed Martin Company, for the United States Department of Energy's National Nuclear Security Administration under Contract DE-AC04-94AL85000.

REFERENCES

1. Herrmann, W., "Constitutive Equation for the Dynamic Compaction of Ductile Porous Materials," *J. Appl. Phys.,* vol. 10, pp. 2490-2499, 1969.
2. Grady, D. E., et al., "Computational modeling and wave propagation in media with inelastic deforming microstructure," *J. Phys. IV,* vol.10, pp.15-20, 2000.
3. Grady, D. E., et al., "A computational model for polyurethane foam," in *Fundamental Issues and Applications of Shock-Wave and High-Strain-Rate Phenomena*, K. P. Staudhammer, L. E. Murr, and M. A. Meyers, Eds., 2001, pp. 485-491.
4. Vogler, T. J., et al., "Static and dynamic compaction of ceramic powders," *Int. J. Sol. St.,* vol. 44, pp. 636-658, 2007.
5. Tsembelis, K., et al., "The behavior of sand under shock wave loading: experiments and simulations," in *DYMAT: Saint-Louis, France*, 2002, pp. 193-203.
6. Lagunov, V. A., et al., "Measuring measurements of the dynamic compressibility of sand," *Zhurnal Prikladnoi Mekhaniki i Tehknicheskoi Fiziki,* vol. 4, pp. 88-96, 1963.
7. M. van Thiel (Ed.), "Compendum of shock wave data," *Lawrence Livermore Laboratory Report UCRL-50108,* 1977.
8. Dianov, M., et al., "Shock compressibility of dry and water-saturated sand," *Soviet Technical Physics Letters,* vol. 2, pp. 207-208, 1976.
9. Swegle, J. W., et al., "Shock viscosity and the prediction of shock wave rise times," *J. App. Phys.,* vol. 58, pp. 692-701, 1985.
10. Anderson, M. U., et al., "Time-resolved shock compression of porous rutile: wave dispersion in porous solids " *In: High-Pressure Science and Technology. AIP, New York,* pp. 1111-1114, 1994.